Bone Reports 17 (2022) 101612

Contents lists available at ScienceDirect

Bone Reports

journal homepage: www.elsevier.com/locate/bonr

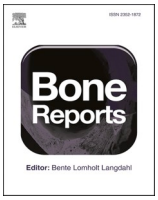

Cortical porosity occurs at varying degrees throughout the skeleton in rats with chronic kidney disease

Corinne E. Metzger [a], Christopher L. Newman [b], Samantha P. Tippen [a], Natalie T. Golemme [a], Neal X. Chen [c], Sharon M. Moe [c], Matthew R. Allen [a,c,d,*]

[a] Department of Anatomy, Cell Biology, and Physiology, Indianapolis, IN, USA, 46202
[b] Department of Radiology and Imaging Sciences, Indianapolis 46202, IN, USA
[c] Department of Medicine, Indiana University School of Medicine, Indianapolis 46202, IN, USA
[d] Department of Biomedical Engineering, Indiana University Purdue University Indianapolis, Indianapolis 46202, IN, USA

ARTICLE INFO

Keywords:
Micro-CT
Cortical porosity
CKD-MBD
Imaging

ABSTRACT

Cortical porosity develops in chronic kidney disease (CKD) and increases with progressing disease. Cortical porosity is likely a prominent contributor to skeletal fragility/fracture. The degree to which cortical porosity occurs throughout the skeleton is not fully known. In this study, we assessed cortical bone porosity via micro-computed tomography at multiple skeletal sites in rats with progressive chronic kidney disease. We hypothesized that cortical porosity would occur in long bones throughout the body, but to a lesser degree in flat bones and irregular bones. Porosity was measured, using micro-CT, at 17 different skeletal sites in 6 male rats with CKD. Varying degrees of porosity were seen throughout the skeleton with higher porosity in flat and irregular bone (i.e. parietal bone, mandible) vs. long bones ($p = 0.01$) and in non-weightbearing bones vs. weightbearing bones ($p = 0.01$). Porosity was also higher in proximal sites vs. distal sites in long bones ($p < 0.01$ in all comparisons). There was large heterogeneity in porosity within skeletal sites across rats and within the same rat across skeletal sites. Correlations showed cortical porosity of the proximal tibia was positively associated with porosity at the other sites with the strongest correlation to the parietal bone and the weakest to the ulna. Overall, our data demonstrates varying and significant cortical bone porosity across the skeleton of animals with chronic kidney disease. These data point to careful selection of skeletal sites to assess porosity in pre-clinical studies and the potential for fractures at multiple skeletal sites in patients with CKD.

1. Introduction

Chronic kidney disease (CKD), a disease characterized by progressive declines in kidney function, has a global prevalence of approximately 9 % which amounts to ~700 million cases (Cockwell and Fisher, 2020). The prevalence is ~15 % in US adults (Centers for Disease Control and Prevention, 2021). Mineral metabolism dysregulation, high circulating parathyroid hormone, and accumulation of uremic toxins in CKD lead to dramatic loss of bone and increased fracture risk. A particular hallmark of bone loss in CKD is cortical bone deterioration. While cortical thinning contributes to loss of cortical bone, cortical porosity, excavated holes in cortical bone caused by rampant bone resorption, is prominent and has a major negative impact on the structural integrity of the skeleton. Both clinical and pre-clinical studies have shown that cortical porosity development occurs rapidly with advancing kidney disease (Nickolas et al., 2013; Mcnerny et al., 2019; Metzger et al., 2019). Over approximately 2 years, cortical porosity had the greatest percent change from baseline (4 %) compared to other cortical parameters in patients with CKD in both the distal radius and the distal tibia (Nickolas et al., 2013).

This loss of cortical bone in CKD positively correlates with fracture rate. Patients with CKD have significantly higher rates of fracture at all ages compared to healthy individuals and the incidence of fracture increases with declining kidney function (Naylor et al., 2014). Hip fracture rates, the most clinically relevant site, are high in CKD compared to the general population (Alem et al., 2000; Nickolas et al., 2006). However, fractures occur at other skeletal sites in CKD patients as well (Naylor et al., 2014; Ambrus et al., 2011; Iimori et al., 2012) and a large portion

* Corresponding author at: Department of Anatomy, Cell Biology, & Physiology, Indiana University School of Medicine, 635 Barnhill Drive, MS 5045, Indianapolis, IN 46202, USA.
E-mail address: matallen@iu.edu (M.R. Allen).

https://doi.org/10.1016/j.bonr.2022.101612
Received 1 April 2022; Received in revised form 3 June 2022; Accepted 15 August 2022
2352-1872/Published by Elsevier Inc. This is an open access article under the CC BY-NC-ND license (http://creativecommons.org/licenses/by-nc-nd/4.0/).

of these fractures are in non-hip cortical bone sites (Moe et al., 2015a). Studies have demonstrated that small changes in porosity significantly impact the mechanical properties of bone (Currey, 1988; Schaffler and Burr, 1988). In cadaver cortical bone specimens, porosity accounted for 76 % of the reduction in strength of the samples when mechanically tested while mineral content had little effect (McCladen et al., 1993). While porosity likely plays a major role in fracture rates/risks in CKD, knowledge regarding porosity across the skeleton is limited.

In clinical studies, cortical porosity is typically measured at the distal tibia or distal radius as both sites are accessible via high resolution quantitative peripheral computed tomography (HR-pQCT) or at the iliac crest from a bone biopsy. In rodent studies, cortical porosity is routinely measured via micro-computed tomography at the tibia (distal or proximal) or the distal/midshaft femur. Previous studies have demonstrated associations between parameters from HR-pQCT of distal long bone sites and transiliac crest biopsies in CKD patients, particularly in trabecular bone parameters; however, these studies do not specifically look at porosity (Marques et al., 2017; Cohen et al., 2010). Thus, it is unknown if porosity is similar across various types of bones and different parts of the skeleton. This has important implications for broad assessment of skeletal fragility/fracture risk in patients with CKD as well as enlightening pre-clinical research which typically assesses porosity at a single skeletal site and extrapolates it globally. Therefore, the goal of this project was to assess cortical porosity at multiple skeletal sites in rats with progressive CKD. We hypothesized that cortical porosity would occur in long bones throughout the body, but to a lesser degree in flat bones (i.e. parietal bone and ribs) and irregular bones (mandible).

2. Methods

2.1. Animals

Male autosomal dominant Cy/$+_{IU}$ rats (CKD) progressively develop kidney dysfunction and characteristics of CKD-Mineral Bone Disorder (CKD-MBD) between 28 and 35 weeks of age with cortical porosity developing between 30 and 35 weeks (Mcnerny et al., 2019). Female Cy/+ rats do not develop a similar CKD phenotype (Vorland et al., 2019) and, therefore, only males are typically used to assess alterations due to reduced kidney function in this model. For this study, 6 CKD rats were utilized with 1 age-matched wildtype littermate (CON) for control comparisons. Based on our experience with control rats with normal kidney function across multiple experiments, cortical porosity at this age is minimal (see Supplemental Table).

Bones for this study were obtained from a larger imaging study where rats received one *in vivo* micro-CT scan and one *in vivo* MRI scan of the lower leg; rats received no other treatments. Rats were bred in-house and divided into CKD or CON by plasma blood urea nitrogen measured at 10 weeks of age by colorimetric assay (BioAssay Systems, Hayward, CA, USA). Rats were singly housed throughout the duration of the study in a facility with 12-h light/dark cycles. At 24 weeks of age, all rats were switched to a purified casein-based diet with 0.7 % phosphorus and 0.7 % calcium (Envigo, Madison, WI, USA). Food and water were provided *ad libitum* throughout the entire study. Rats were maintained on the diet until 33–35 weeks of age when they were euthanized via inhaled carbon dioxide followed by thoracotomy. No blood for serum assays was collected from the parent protocol. All animal procedures were approved by the Indiana University School of Medicine Institutional Animal Care and Use Committee prior to the initiation of any experimental protocols (Study #18072*)*.

2.2. Micro-computed tomography

From each rat, the proximal tibia, distal tibia, midshaft femur, femoral neck, ilium, midshaft humerus, distal radius and ulna, metatarsals, and mandible were scanned on a SkyScan 1172 (Bruker, Billerica, MA, USA) with a 0.5 aluminum filter and a 12 μm voxel size. Ribs (rib number ~ 4–6) and the clavicle were scanned at an 8 μm voxel size. All bones were from the right side of the animal. The right and left parietal bones were scanned at 14 μm voxel size. The choice of voxel size for each set of bones was a balance between bone size and scanning field.

2.3. Cortical porosity assessment

Micro-CT scans were reconstructed with Bruker software (NRecon) with smoothing level 2 with a Gaussian smoothing kernel, position 8 ring artifact reduction, and 20 % beam-hardening correction. All samples were reconstructed at a dynamic image range of 0.0 to 0.09. Following reconstruction, scans were rotated to a standard orientation for each bone site (DataViewer; Bruker). Specific anatomical landmarks on bones were utilized to generate standard sites across all the samples.

Proximal tibia shaft: 7 mm below the distal end of the proximal growth plate.
Distal tibia shaft: 4 mm distal to the tibiofibular junction.
Femoral neck: immediately proximal to the separation from the proximal shaft.
Midshaft femur: 5 mm distal to the end of the ridge of the third trochanter.
Distal radius and ulna shaft: 6 mm proximal to the distal end of the bone pair.
Distal humerus shaft: 11 mm from distal end of bone.
Medial clavicle: 3 mm from medial end.
Metatarsals: 2 mm from proximal end of the first metatarsal.
Ilium: 7 mm cephalad to the acetabulum.
Rib: 5 mm from medial end.
Mandible: at the midpoint of the most caudal tooth.
Parietal bones: 4 mm posterior to the coronal suture.

Outcome parameters were assessed from hand drawn regions of interest of five contiguous slices tracing the periosteal and endosteal surfaces. Bone volume was measured including the void spaces (pores) between the periosteal and endosteal surfaces. Cortical porosity was defined as the inverse of bone volume or the percent of void space within the cortical bone region (i.e. 95 % bone volume = 5 % cortical porosity). (Supplemental Fig. 1). A single average value from the five slices was obtained. The mandibular canal was removed from the region of interest in the mandible. The sagittal suture was included in the region of interest for the parietal bone (Supplemental Fig. 2). The supplemental table has all cortical porosity values, as a percent of total cortical bone area.

Further regions of interest were obtained from the proximal tibia, distal tibia, proximal femur, and midshaft femur scans with regions of interest selected approximately 4 mm apart to capture 7 regions within the tibia and 4 regions within the femur to assess porosity changes across the length of the bone.

2.4. Statistical analyses

Data were grouped by site and by rat and graphed to demonstrate the range of porosity both within site and within rat. Each site in CKD rats was correlated to proximal tibia porosity (the site our group traditionally uses in this rodent model) and Spearman's *r* was recorded. As the goal of the work was to examine differences across sites in CKD, not to compare CKD to control (which has been well-established in the literature) the control sample was not included in any of the analyses or correlations. Several statistical comparisons were made across CKD rats excluding the control sample: Paired *t*-tests were performed to compare distal vs. proximal sites (proximal tibia vs. distal tibia; femoral neck vs. midshaft femur; midshaft humerus vs. distal radius) within CKD rats. Paired t-tests were also utilized to assess forelimb vs. hindlimb porosity (midshaft femur vs. midshaft humerus: distal tibia vs. distal radius) within CKD rats. To assess whether there are differences between

weightbearing and non-weightbearing bone sites, we were unable to do a paired *t*-test; instead, we pulled together weightbearing sites (tibia, femur, radius, ulna, humerus) and non-weightbearing sites (clavicle, rib, mandible, parietal bone) within CKD rats and performed a Mann-Whitney *U* test. Likewise, we utilized the Mann-Whitney U test to compare long bones (midshaft femur, proximal and distal tibia, humerus, radius, ulna) and flat/irregular bones (ilium, rib, parietal, mandible) within CKD rats. $p < 0.05$ was considered statistically significant. All statistical tests were completed on SPSS Statistics version 28 (IBM; Armonk, NY, USA). Data for statistical tests are presented as individual data points with the error bar as standard deviation.

3. Results

3.1. Descriptive statistics of cortical porosity within CKD rats

The range of cortical porosity in the appendicular skeleton of CKD animals, excluding the metatarsals, was greatest in the proximal tibia (12.5 % to 59.8 %) and at lowest at the ulna (0.6 % to 3.3 %; Figs. 1, 2, 4a). The average cortical porosity in the CKD animals in the appendicular skeleton was highest in the femoral neck (42.4 % ± 16.7) and lowest in the ulna (1.9 % ± 0.9). Within the axial skeleton, the rib had the greatest range in cortical porosity (2.8 % to 65.1 %) with the mandible having the lowest range (29.6 % to 72.4 %; Figs. 3, 4A). The highest average porosity in the axial skeleton was in the parietal bone (49.75 % ± 20.6) and the lowest in the rib (25.0 % ± 24.8). Within the five metatarsals, the first metatarsal had the highest range (3.1 % to 33.7 %) and the highest average (14.6 % ± 12.3) while the second metatarsal had the lowest range (0.4 % to 1.2 %) and the lowest average porosity (0.7 % ± 0.4; Fig. 5a, b). Of all sites measured, the site with the highest average porosity was the parietal bone (49.8 % ± 20.6) followed by the mandible (47.0 % ± 17.0) followed by the femoral neck (42.4 % ± 16.7). Within rats including all bone sites, excluding the metatarsals, CKD1 had the highest range (3.3 % to 84.5 %) and the greatest average total body cortical porosity (43.5 % ± 24.2; Fig. 6). CKD4, the rat with the lowest range (1.3 % to 29.6 %), also had the lowest total average porosity (13.8 % ± 11.8; Fig. 6). Table 1 has cortical porosity values, as a percent of total cortical bone area, for all bone sites across all CKD animals.

3.2. Porosity across the tibia and femur

From seven regions selected across the two tibia scans, porosity was higher at the proximal tibia compared to porosity at the midshaft or below (Fig. 7). Across 4 regions in the femur, the femoral neck had higher porosity than other sites along the proximal and midshaft femur (Fig. 8).

3.3. Bone site comparisons

In a paired *t*-test, the distal tibia had less porosity than the proximal tibia ($p = 0.01$). Similarly, the proximal femur had higher porosity than the midshaft femur ($p = 0.019$) and the midshaft humerus had higher porosity than the distal radius ($p < 0.0001$; Fig. 9a). Comparing hindlimb and forelimb, there was no statistical difference between cortical porosity in the midshaft femur and midshaft humerus ($p = 0.088$), but the distal tibia did have higher porosity than the distal radius ($p = 0.004$; Fig. 9b). Grouping together long bone sites and flat/irregular bone sites, flat and irregular bones had higher cortical porosity than did long bones ($p < 0.0001$; Fig. 9c). Comparing weight-bearing sites vs. non-weightbearing sites, non-weightbearing sites had higher porosity than did weight bearing sites ($p = 0.01$; Fig. 9d).

3.4. Correlations across bone sites

CKD rat proximal tibia cortical porosity was correlated to all bone sites measured excluding metatarsals 2–5. The strongest correlations were to the parietal bone ($r = 0.995$), the rib ($r = 0.990$), the mandible ($r = 0.985$), and the distal tibia ($r = 0.985$). The weakest correlations were to the ulna ($r = 0.562$) and the femoral neck ($r = 0.671$; Fig. 10).

4. Discussion

The primary finding of this study is that cortical porosity occurs at varying degrees throughout the skeleton of rats with CKD with the most prevalent porosity in the axial skeleton and the long bones of the

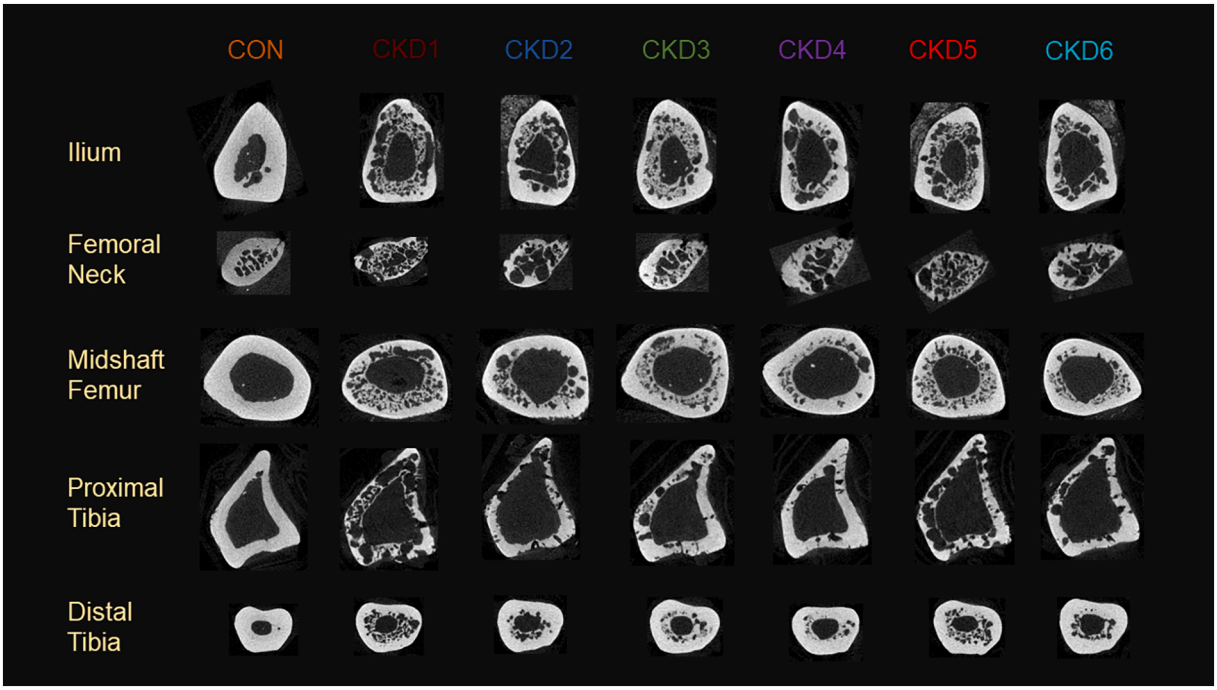

Fig. 1. Images of micro-CT scans of hindlimbs – ilium, femoral neck, midshaft femur, proximal tibia, distal tibia.

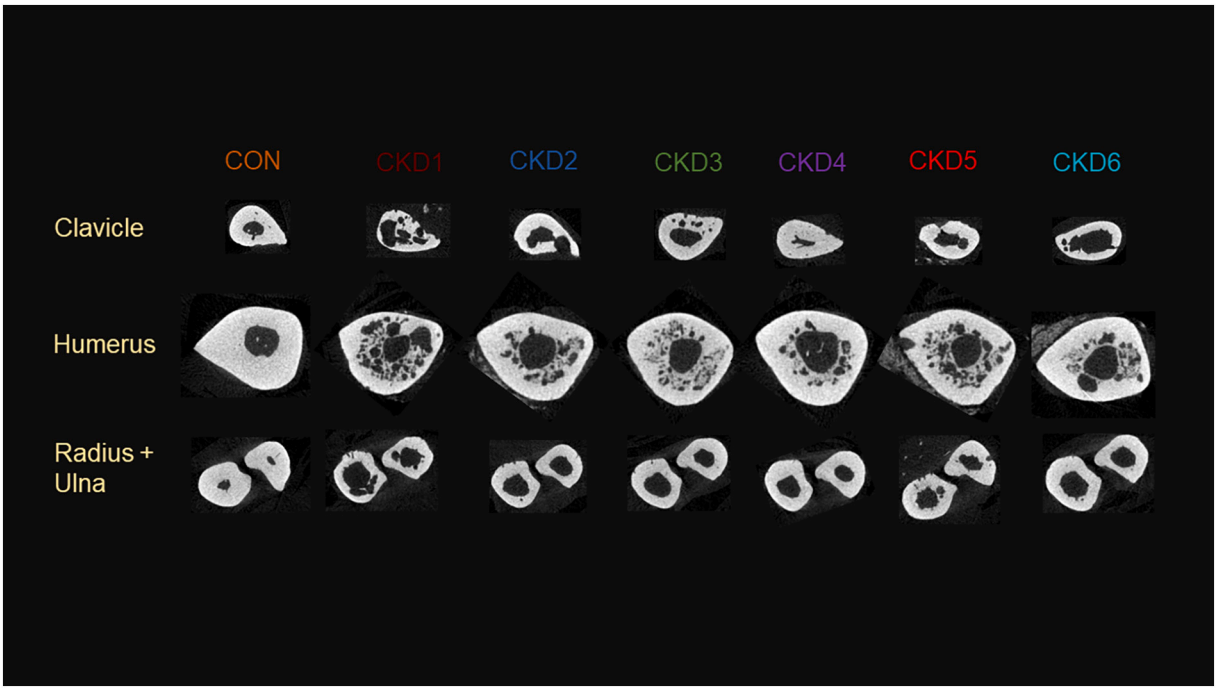

Fig. 2. Micro-CT images from scans of forelimbs – clavicle, humerus, radius and ulna.

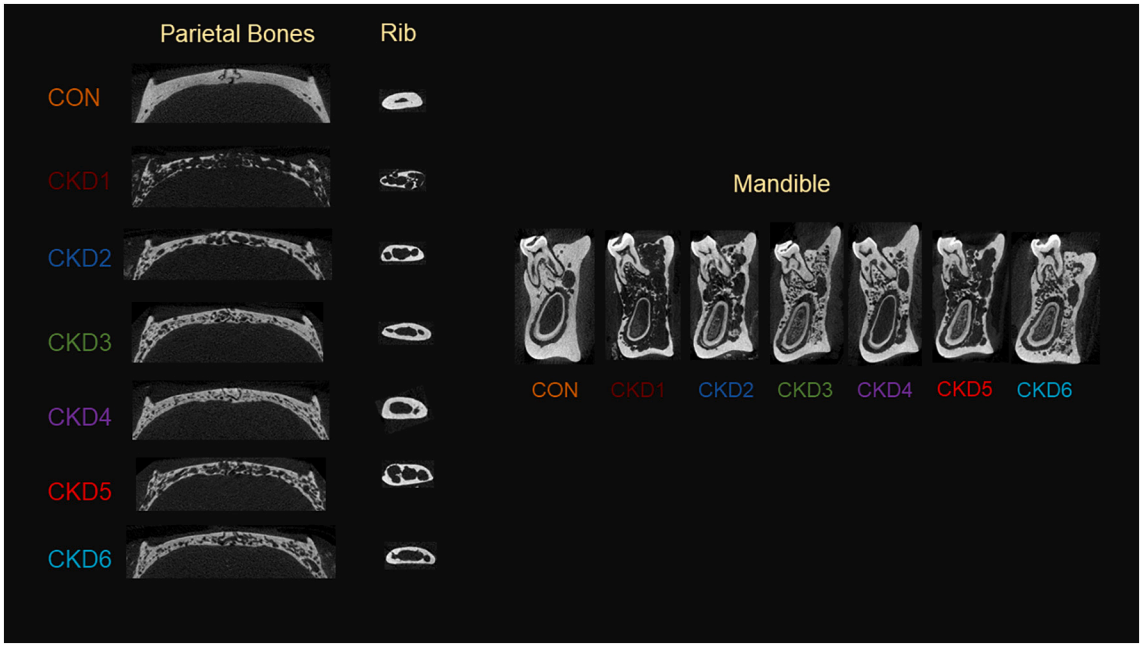

Fig. 3. Images of micro-CT scans of the axial skeleton – parietal bones, rib, and mandible.

hindlimb. Contrary to our original hypothesis, flat and irregular bones had higher cortical porosity than long bone sites measured. Additionally, the skeletal location (i.e., proximal vs. distal) had a significant impact on cortical porosity prevalence. Within rats, the heterogeneity of porosity was large across the sites measured demonstrating the variability of cortical bone deterioration across the skeleton.

In clinical studies, hip fractures are often the primary concern due to the high morbidity and mortality associated with their occurrence and, therefore, are the most reported fracture site. Hip fractures are higher in CKD patients vs. the general population (Kim et al., 2016), higher in patients requiring dialysis (Alem et al., 2000; Maravic et al., 2014; Tentori et al., 2014), and generally increase in prevalence with increasing stages of CKD (Nickolas et al., 2006; Pimentel et al., 2017). While less reported, fractures in other skeletal sites have also been noted. For example, in one cohort of patients on maintenance dialysis, 24 % of fractures were in the leg, 24 % in the forearm, and 14 % in the hip (Ambrus et al., 2011). In another group of dialysis patients, 23 % of fractures noted were in the hip, 21 % in the clavicle or rib, while 13 % were in the tibia/fibula and in the wrist (Iimori et al., 2012). In a study of 3883 dialysis patients with secondary hyperparathyroidism, over 50 % of the adjudicated fractures were at non-hip cortical sites (Moe et al., 2015a). Unfortunately, in these studies, cortical porosity was not

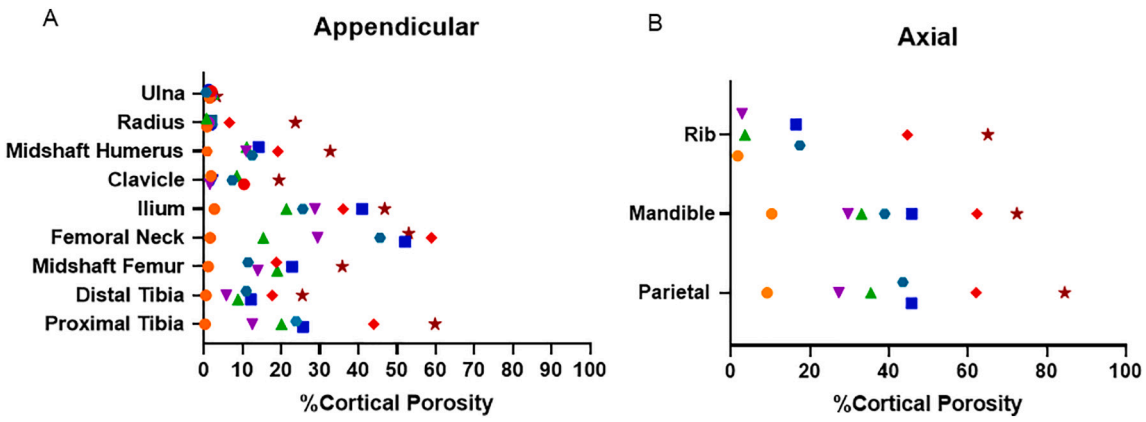

Fig. 4. Spread of cortical porosity in the appendicular (A) and axial (B) skeleton across all rats. Data points of the same color and shape refer to the same rat (i.e. orange circles = CON).

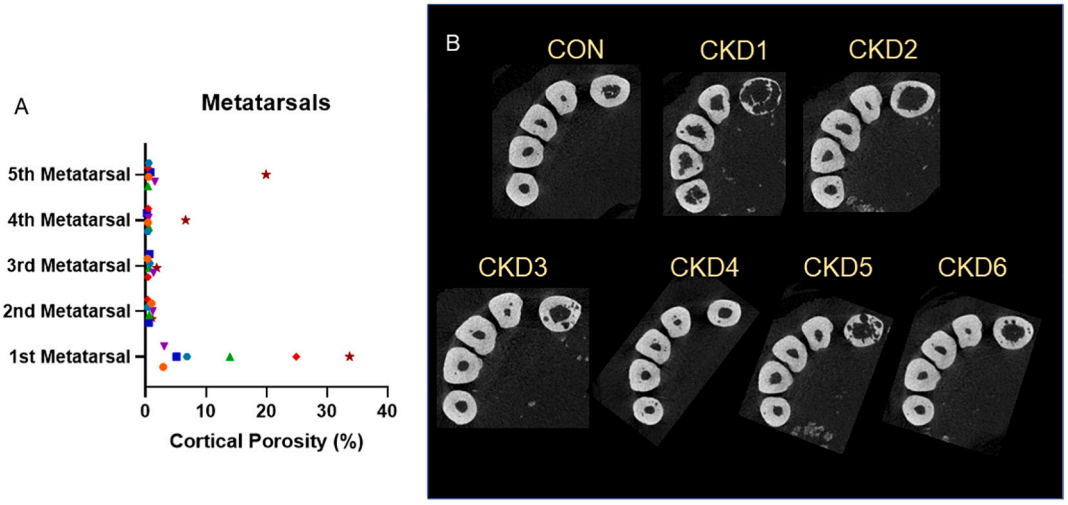

Fig. 5. Spread of cortical porosity in the metatarsals across all rats (A) and images from the micro-CT scans (B). Data points of the same color and shape refer to the same rat (i.e. orange circles = CON).

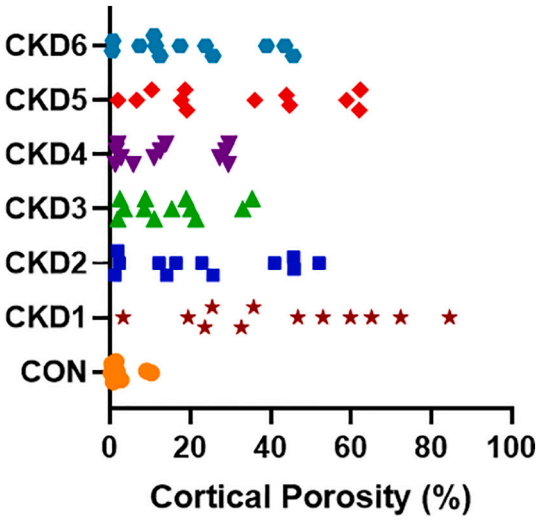

Fig. 6. Cortical porosity spread within the same rat at all skeletal sites measured excluding the metatarsals. Data points of the same color and shape all refer to the same rat.

Table 1
Cortical porosity (%) in all rats at all bone sites.

Site	CKD1	CKD2	CKD3	CKD4	CKD5	CKD6	CON
Proximal tibia	59.84	25.66	20.09	12.50	43.95	23.83	0.27
Distal tibia	25.49	12.18	8.81	5.79	17.68	10.95	0.49
Midshaft femur	35.82	22.86	18.97	13.90	18.71	11.41	1.05
Femoral neck	53.05	52.07	15.38	29.45	58.91	45.61	1.60
Ilium	46.80	40.95	21.36	28.76	36.08	25.60	2.68
Clavicle	19.44	2.29	8.51	1.53	10.39	7.34	1.85
Midshaft humerus	32.70	14.16	11.08	10.96	19.14	12.48	0.77
Radius	23.66	1.92	1.94	1.27	6.62	0.69	0.80
Ulna	3.27	1.20	2.48	1.92	1.94	0.57	1.49
1st Metatarsal	24.90	5.13	13.96	3.08	33.73	6.85	2.90
2nd Metatarsal	1.17	0.56	0.63	1.19	0.36	0.35	0.97
3rd Metatarsal	1.86	0.65	0.59	1.33	0.43	0.68	0.32
4th Metatarsal	6.60	0.21	0.51	0.50	0.46	0.36	0.38
5th Metatarsal	19.93	0.83	0.39	1.56	0.37	0.53	0.49
Parietal Bone	84.52	45.74	35.40	27.28	62.07	43.56	9.12
Mandible	72.41	45.83	33.06	29.63	62.30	38.93	10.28
Rib	65.09	16.46	3.50	2.80	44.69	17.42	1.72

measured. Cortical porosity tends to increase with advancing stages of CKD and fracture risk increases significantly with decline in kidney function (Naylor et al., 2014). Interestingly, Naylor et al. tracked the first fracture reported accounting for stage of kidney function and found

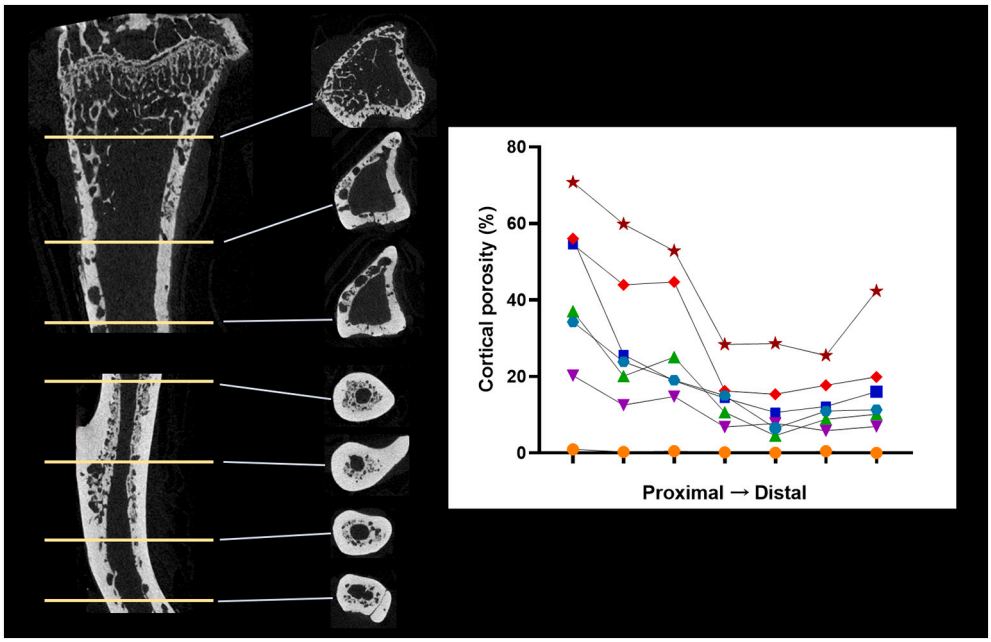

Fig. 7. Cortical porosity assessed at seven sites across the proximal to distal tibia.

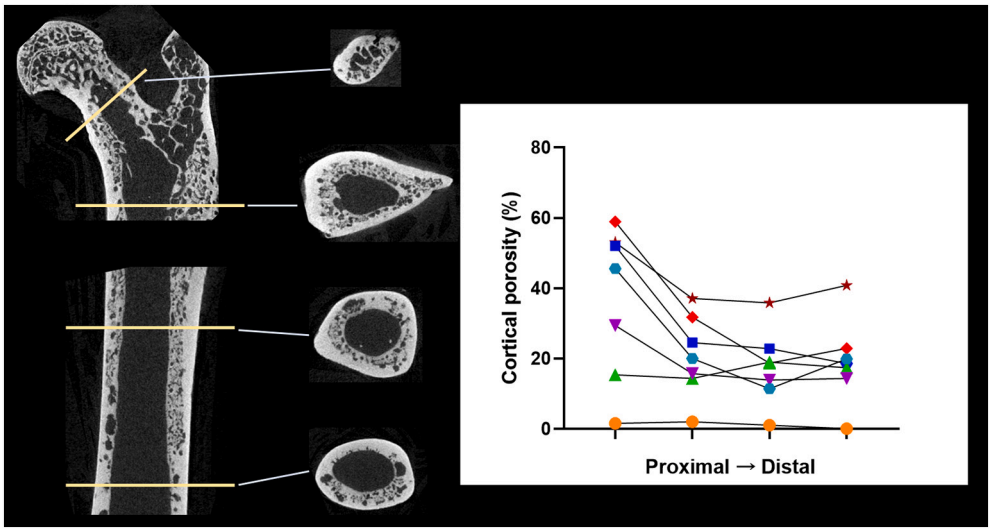

Fig. 8. Cortical porosity assessed at four different sites from the proximal through midshaft femur.

that 47 % of first fractures for those with normal kidney function were in the forearm, while 27 % were in the hip; however, in individuals with the lowest kidney function, hip fractures accounted for 54 % of total fractures and forearm fractures accounted for 19 % (Naylor et al., 2014). Generally, first fracture sites of the arm decreased with declines in kidney function while hip fractures increased with declines in kidney function (Naylor et al., 2014). While the reasons for this are not hypothesized by the authors, it is plausible that increased cortical porosity with advancing CKD could weaken the femoral neck leading to an increase in fractures at this site while fall-related fractures at the forearm decreased. Although measuring in rodents which are quadrupeds, the femoral neck site had the greatest average porosity across the appendicular sites we assessed. Development of techniques to image the femoral neck/hip for porosity in human clinical patients could be advantageous for assessing patients at risk for hip fractures.

Despite differences in cortical bone structure and physiology between humans and rodents, both develop cortical porosity in several different conditions including CKD (Nickolas et al., 2013; Mcnerny et al., 2019; Metzger et al., 2021a). Therefore, we hypothesize there are similar mechanisms initiating porosity development despite a lack of basal intracortical remodeling in rats. The Cy rat model of CKD leads to significant and rapid porosity development between 30 and 35 weeks of age (Mcnerny et al., 2019). Typically, rodent studies measure cortical porosity at a single site, often at the tibia or femur. In this study, we examined porosity at multiple sites throughout the rat skeleton and found porosity varied significantly across sites within rats and within rats across sites. Bones of the hindlimb tended to have higher porosity than bones of the forelimb. Additionally, within the metatarsals, porosity was present at the site measured in the 1st metatarsal of CKD rats, but rarely present in metatarsals 2–5. We also found higher porosity at proximal sites vs. distal sites in paired *t*-tests within animals and higher porosity in non-weightbearing sites vs. weightbearing sites in pooled samples. Therefore, the site or sites measured in pre-clinical rodent studies should be carefully considered when making general

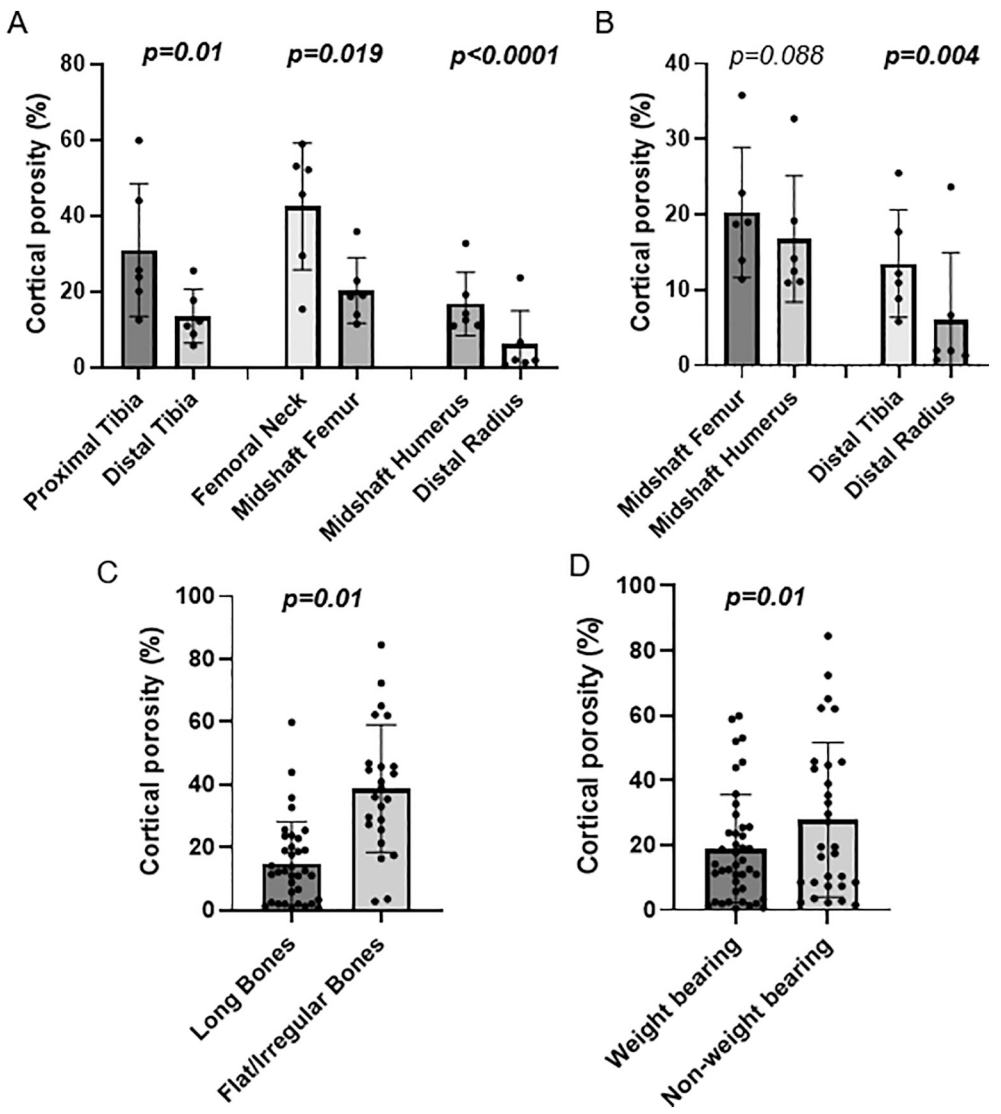

Fig. 9. Comparisons of cortical porosity across skeletal sites. A) Cortical porosity was higher in proximal sites vs. distal sites at the proximal and distal tibia, femoral neck and midshaft femur, and midshaft humerus and distal radius. B) Cortical porosity was not statistically higher in the midshaft femur vs. the midshaft humerus, but porosity was higher in the distal tibia vs. the distal radius. C) Flat and irregular bones had higher porosity than long bones. D) Non-weightbearing sites had higher porosity than weightbearing skeletal sites. The p-value of each independent test is listed.

conclusions about the data. For example, external loading studies in rodents to assess the impact of mechanical loading are often completed on the ulna; however, if porosity was a primary outcome of interest, utilizing this site may limit conclusions due to less porosity at that site. Within our data, the proximal tibia, a site routinely used by us and others to examine bone morphology, correlated with most other sites, albeit to varying degrees. Interestingly, we found significant cortical porosity at sites typically not assessed, like the parietal bone and mandible, which may indicate the need for increased understanding of cortical bone changes in CKD at sites beyond the hip and long bones and how this may lead to other complications associated with the skeleton. For example, expansive jaw lesions have been documented in CKD patients as well as radiographic evidence of calvaria bone deterioration (Raubenheimer et al., 2015). These clinical findings, consistent with the findings in our rodents, demonstrate the rodent model as reflective of human disease.

While not empirically studied here, we speculate several potential factors that could influence the variation in cortical porosity across the skeleton. First, it is plausible that mechanical loads could have an impact on where and to what degree pores develop. While the relationship between porosity and mechanical loading is not known, greater mechanical loads on a site could potentially prevent or lessen pore development. On the contrary, increased loads, particularly fatigue-inducing loads, could increase damage within the bone leading to an increased need to remodel, therefore, increasing porosity. Statistically, there was higher porosity in non-weightbearing sites when compared to weightbearing sites. Within weight bearing sites, distal tibia had higher porosity than the distal radius. Studies examining the normal load bearing of rats have demonstrated that ~80 % of their body weight is placed on their hindlimbs while standing (Schött et al., 1994) and approximately 50 % is carried on the forelimbs and hindlimbs each while normally ambulating (Clarke, 1995). The rats in our study had normal weightbearing loads without additional activity so we cannot assume increased mechanical forces lead to porosity changes. Due to the normal weight-bearing of standing bearing more on the hindlimbs, we also cannot assume the forelimb has less porosity due to increased mechanical loads. Secondly, our group has previously demonstrated that higher cortical bone blood perfusion was associated with higher cortical porosity in the femur and tibia (Aref et al., 2019). In healthy standing rats, bone blood perfusion is higher in sites like the proximal tibia and femoral neck than in sites like the distal tibia and distal radius/ulna (Colleran et al., 2000). Therefore, we speculate differences in bone vascular perfusion could potentially have an impact on porosity variation. Finally, we have previously assessed osteocyte apoptosis and osteocyte RANKL in rodents with CKD hypothesizing that alterations in osteocyte lifespan and signaling could instigate osteoclast resorption of cortical bone (Metzger et al., 2019; Metzger et al., 2021b). Therefore, we speculate that differences in osteocyte density or signaling across sites of

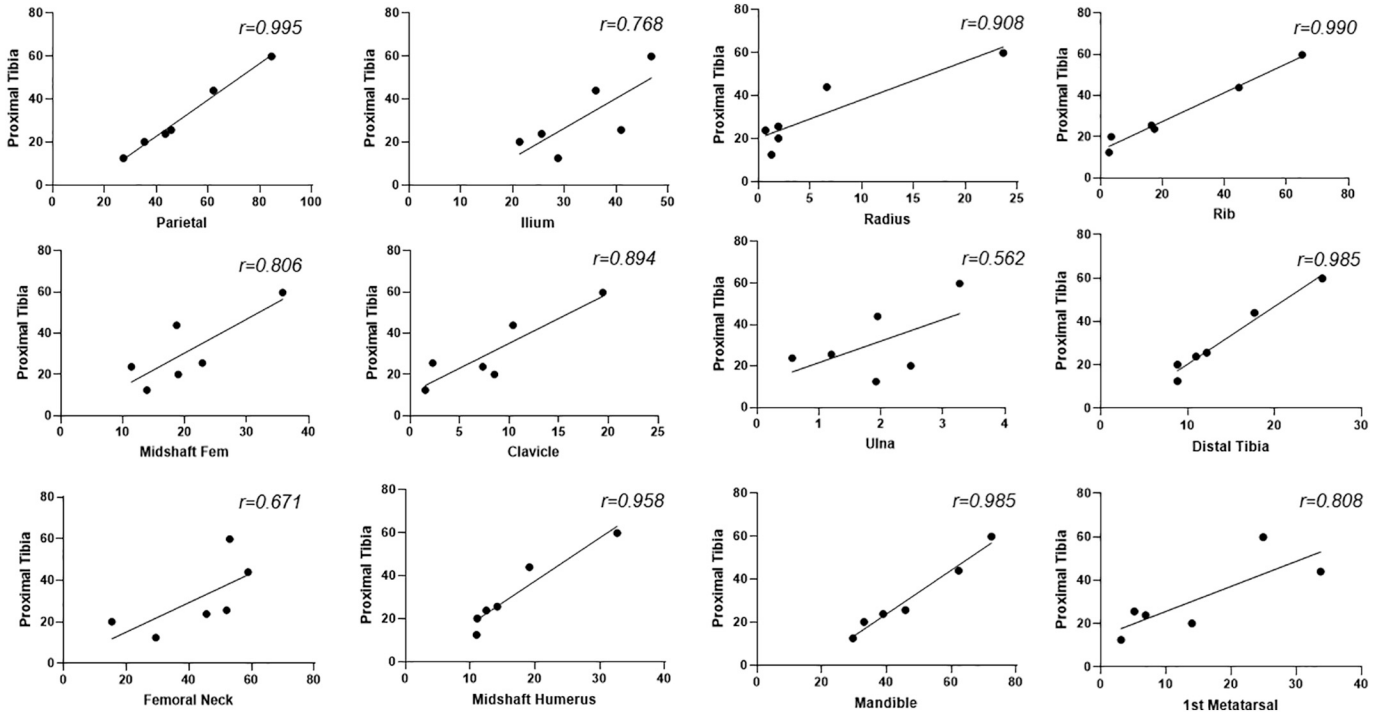

Fig. 10. Correlations between proximal tibia cortical porosity and other skeletal sites. The *r* correlation coefficient is reported in the top right of each graph.

the skeleton may also be a contributing factor to the variation in cortical porosity.

This study is limited in that we are unable to directly assess severity of CKD in the rodents studied as no serum/plasma was collected at study endpoint in the parent protocol to measure markers of kidney function or parathyroid hormone (PTH); however, previous work with this same model of rats consistently demonstrates high circulating PTH and decreased kidney function by the age of the animals in this study (Mcnerny et al., 2019; Moe et al., 2014; Moe et al., 2015b; Allen et al., 2020; Moe et al., 2009; Chen et al., 2020). Furthermore, we were unable to assess bone turnover due to tissues from the parent protocol not being stored for histology. CKD with high circulating PTH, which the Cy/+ male rats demonstrate, is characterized by high bone turnover in both rodent (Metzger et al., 2021a; Metzger et al., 2021b; Moe et al., 2014; Moe et al., 2015b; Chen et al., 2020) and clinical studies (Malluche et al., 2011). While unable to directly assess bone turnover in this study, previous work consistently demonstrates high bone turnover in these CKD rats (Moe et al., 2014; Moe et al., 2015b; Chen et al., 2020); however, we cannot assess differences between animals in this study or relate turnover to cortical porosity. Additionally, a sex comparison is not possible with this model of progressive CKD due to heterozygous female Cy/+ rats not developing features of kidney disease, but other models, like adenine-induced CKD, could be used for this type of assessment in the future. Our scanning voxel size in this study, while sufficient to detect the macro porosity present in these rats, may not detect much smaller micro-level pores. Furthermore, future studies can assess the mechanistic drivers of cortical deterioration across the skeleton. Finally, the rats in our study were all approximately the same age so we cannot determine if there are temporospatial aspects that factor into cortical porosity initiation or if the speed of progression differs among sites.

In conclusion, cortical porosity occurs throughout the skeleton in rats with progressive CKD. There is variation both across individuals within skeletal sites and across skeletal sites within an individual rat. From a pre-clinical study perspective, these data demonstrate that porosity assessment at only one site of the skeleton may not be generalizable to the skeleton as a whole and the location of the site(s) measured could influence the interpretation of the data. Additionally, care should be taken to assess cortical porosity in the same region as other tests, particularly those looking at mechanical properties of bone. From a clinical perspective, these data in a rodent model of CKD demonstrate the potential for porosity-related weakening of bones at multiple skeletal sites in patients with CKD.

Supplementary data to this article can be found online at https://doi.org/10.1016/j.bonr.2022.101612.

Funding

This work was supported by a United States (U.S.) Department of Veterans Affairs Merit Grant (BX003025) to MRA, RSNA Research & Education Foundation (075717-00002B) to CLN, NIH (F32DK122731) to CEM and NIH grant (R01DK110871) to SMM/MRA. The contents do not represent the views of the NIH, U.S. Department of Veterans Affairs or the United States Government or the RSNA R&E Foundation.

Data availability

All data utilized in this manuscript is presented in table or graph format.

CRediT authorship contribution statement

Corinne E. Metzger: Conceptualization, Data curation, Formal analysis, Investigation, Validation, Writing – original draft, Writing – review & editing. **Christopher L. Newman:** Funding acquisition, Validation, Writing – review & editing. **Samantha P. Tippen:** Conceptualization, Investigation, Writing – review & editing. **Natalie T. Golemme:** Data curation, Formal analysis, Investigation, Writing – review & editing. **Neal X. Chen:** Resources, Writing – review & editing. **Sharon M. Moe:** Resources, Writing – review & editing. **Matthew R. Allen:** Conceptualization, Formal analysis, Funding acquisition, Project administration, Resources, Supervision, Writing – review & editing.

Declaration of competing interest

The authors have no conflicts of interest.

References

Alem, A.M., Sherrard, D.J., Gillen, D.L., Weiss, N.S., Beresford, S.A., Heckbert, S.R., Wong, C., Stehman-Breen, C., 2000. Increased risk of hip fracture among patients with end-stage renal disease. Kidney Int. 58, 396–399. https://doi.org/10.1046/j.1523-1755.2000.00178.x.

Allen, M.R., Wallace, J., McNerney, E., Nyman, J., Avin, K., Chen, N., Moe, S., 2020. N-acetylcysteine (NAC), an anti-oxidant, does not improve bone mechanical properties in a rat model of progressive chronic kidney disease-mineral bone disorder. PLoS One 15, 1–11. https://doi.org/10.1371/journal.pone.0230379.

Ambrus, C., Almasi, C., Berta, K., Deak, G., Marton, A., Molnar, M.Z., Nemeth, Z., Horvath, C., Lakatos, P., Szathmari, M., Mucsi, I., 2011. Vitamin D insufficiency and bone fractures in patients on maintenance hemodialysis. Int. Urol. Nephrol. 43, 475–482. https://doi.org/10.1007/s11255-010-9723-x.

Aref, M.W., Swallow, E.A., Metzger, C.E., Chen, N., Moe, S.M., Allen, M.R., 2019. Parathyroid suppression therapy normalizes chronic kidney disease-induced elevations in cortical bone vascular perfusion: a pilot study. Osteoporos. Int. 30, 1693–1698. https://doi.org/10.1007/s00198-019-04974-z.

Centers for Disease Control and Prevention, 2021. In: Chronic Kidney Disease in the United States, 2021, 1. CDC, pp. 1–6. https://www.cdc.gov/kidneydisease/publications-resources/2019-national-facts.html.

Chen, N.X., Srinivasan, S., O'Neill, K., Nickolas, T.L., Wallace, J.M., Allen, M.R., Metzger, C.E., Creecy, A., Avin, K.G., Moe, S.M., 2020. Effect of advanced glycation end-products (AGE) lowering drug ALT-711 on biochemical, vascular, and bone parameters in a rat model of CKD-MBD. J. Bone Miner. Res. 35, 608–617. https://doi.org/10.1002/jbmr.3925.

Clarke, K.A., 1995. Differential fore- and hindpaw force transmission in the walking rat. Physiol. Behav. 58, 415–419. https://doi.org/10.1016/0031-9384(95)00072-Q.

Cockwell, P., Fisher, L.A., 2020. The global burden of chronic kidney disease. Lancet 395, 662–664. https://doi.org/10.1016/S0140-6736(19)32977-0.

Cohen, A., Dempster, D.W., Müller, R., Guo, X.E., Nickolas, T.L., Liu, X.S., Zhang, X.H., Wirth, A.J., Van Lenthe, G.H., Kohler, T., McMahon, D.J., Zhou, H., Rubin, M.R., Bilezikian, J.P., Lappe, J.M., Recker, R.R., Shane, E., 2010. Assessment of trabecular and cortical architecture and mechanical competence of bone by high-resolution peripheral computed tomography: comparison with transiliac bone biopsy. Osteoporos. Int. 21, 263–273. https://doi.org/10.1007/s00198-009-0945-7.

Colleran, P.N., Wilkerson, M.K., Bloomfield, S.A., Suva, L.J., Turner, R.T., Delp, M.D., 2000. Alterations in skeletal perfusion with simulated microgravity: a possible mechanism for bone remodeling. J. Appl. Physiol. 89, 1046–1054. https://doi.org/10.1152/jappl.2000.89.3.1046.

Currey, J.D., 1988. The effect of porosity and mineral content on the Young's modulus of elasticity of compact bone. J. Biomech. 21, 131–139. https://doi.org/10.1016/0021-9290(88)90006-1.

Iimori, S., Mori, Y., Akita, W., Kuyama, T., Takada, S., Asai, T., Kuwahara, M., Sasaki, S., Tsukamoto, Y., 2012. Diagnostic usefulness of bone mineral density and biochemical markers of bone turnover in predicting fracture in CKD stage 5D patients-a single-center cohort study. Nephrol. Dial. Transplant. 27, 345–351. https://doi.org/10.1093/ndt/gfr317.

Kim, S.M., Long, J., Montez-Rath, M., Leonard, M., Chertow, G.M., 2016. Hip fracture in patients with non-dialysis-requiring chronic kidney disease. J. Bone Miner. Res. 31, 1803–1809. https://doi.org/10.1002/jbmr.2862.

Malluche, H.H., Mawad, H.W., Monier-Faugere, M.C., 2011. Renal osteodystrophy in the first decade of the new millennium: analysis of 630 bone biopsies in black and white patients. J. Bone Miner. Res. 26, 1368–1376. https://doi.org/10.1002/jbmr.309.

Maravic, M., Ostertag, A., Torres, P.U., Cohen-Solal, M., 2014. Incidence and risk factors for hip fractures in dialysis patients. Osteoporos. Int. 25, 159–165. https://doi.org/10.1007/s00198-013-2435-1.

Marques, I.D.B., Araújo, M.J.C.L.N., Graciolli, F.G., do Reis, L.M., Pereira, R.M., Custódio, M.R., Jorgetti, V., Elias, R.M., David-Neto, E., Moysés, R.M.A., 2017. Biopsy vs. peripheral computed tomography to assess bone disease in CKD patients on dialysis: differences and similarities. Osteoporos. Int. 28, 1675–1683. https://doi.org/10.1007/s00198-017-3956-9.

McCladen, R., McGeough, J., Barker, M., Court-Brown, C., 1993. Age-related changes in the tensile properties of cortical bone. J. Bone Jt. Surg. 75.

Mcnerny, E.M.B., Buening, D.T., Aref, M.W., Chen, N.X., Moe, S.M., Allen, M.R., 2019. Time course of rapid bone loss and cortical porosity formation observed by longitudinal μ CT in a rat model of CKD. Bone 125, 16–24. https://doi.org/10.1016/j.bone.2019.05.002.

Metzger, C.E., Swallow, E.A., Allen, M.R., 2019. Elevations in cortical porosity occur prior to significant rise in serum parathyroid hormone in young female mice with adenine - induced CKD. Calcif. Tissue Int. https://doi.org/10.1007/s00223-019-00642-w.

Metzger, C.E., Swallow, E.A., Stacy, A.J., Allen, M.R., 2021. Adenine-induced chronic kidney disease induces a similar skeletal phenotype in male and female C57BL/6 mice with more severe deficits in cortical bone properties of male mice. PLoS One 16, 1–13. https://doi.org/10.1371/journal.pone.0250438.

Metzger, C.E., Swallow, E.A., Stacy, A.J., Allen, M.R., 2021. Strain-specific alterations in the skeletal response to adenine-induced chronic kidney disease are associated with differences in parathyroid hormone levels. Bone 148, 115963. https://doi.org/10.1016/j.bone.2021.115963.

Moe, S.M., Chen, N.X., Seifert, M.F., Sinders, R.M., Duan, D., Chen, X., Liang, Y., Radcliff, J.S., White, K.E., Gattone, V.H., 2009. A rat model of chronic kidney disease-mineral bone disorder. Kidney Int. 75, 176–184. https://doi.org/10.1038/ki.2008.456.

Moe, S.M., Chen, N.X., Newman, C.L., Gattone, V.H., Organ, J.M., Chen, X., Allen, M.R., 2014. A comparison of calcium to zoledronic acid for improvement of cortical bone in an animal model of CKD. J. Bone Miner. Res. 29, 902–910. https://doi.org/10.1002/jbmr.2089.

Moe, S.M., Abdalla, S., Chertow, G.M., Parfrey, P.S., Block, G.A., Correa-Rotter, R., Floege, J., Herzog, C.A., London, G.M., Mahaffey, K.W., Wheeler, D.C., Dehmel, B., Goodman, W.G., Drüeke, T.B., 2015. Effects of cinacalcet on fracture events in patients receiving hemodialysis: the EVOLVE trial. J. Am. Soc. Nephrol. 26, 1466–1475. https://doi.org/10.1681/ASN.2014040414.

Moe, S.M., Chen, N.X., Newman, C.L., Organ, J.M., Kneissel, M., Kramer, I., Gattone, V. H., Allen, M.R., 2015. Anti-sclerostin antibody treatment in a rat model of progressive renal osteodystrophy. J. Bone Miner. Res. 30, 539–549. https://doi.org/10.1002/jbmr.2372.

Naylor, K.L., McArthur, E., Leslie, W.D., Fraser, L.A., Jamal, S.A., Cadarette, S.M., Pouget, J.G., Lok, C.E., Hodsman, A.B., Adachi, J.D., Garg, A.X., 2014. The three-year incidence of fracture in chronic kidney disease. Kidney Int. 86, 810–818. https://doi.org/10.1038/ki.2013.547.

Nickolas, T.L., McMahon, D.J., Shane, E., 2006. Relationship between moderate to severe kidney disease and hip fracture in the United States. J. Am. Soc. Nephrol. 17, 3223–3232. https://doi.org/10.1681/ASN.2005111194.

Nickolas, T.L., Stein, E.M., Dworakowski, E., Nishiyama, K.K., Komandah-Kosseh, M., Zhang, C.A., McMahon, D.J., Liu, X.S., Boutroy, S., Cremers, S., Shane, E., 2013. Rapid cortical bone loss in patients with chronic kidney disease. J. Bone Miner. Res. 28, 1811–1820. https://doi.org/10.1002/jbmr.1916.

Pimentel, A., Ureña-Torres, P., Zillikens, M.C., Bover, J., Cohen-Solal, M., 2017. Fractures in patients with CKD—diagnosis, treatment, and prevention: a review by members of the european calcified tissue society and the european renal Association of Nephrology Dialysis and Transplantation. Kidney Int. 92, 1343–1355. https://doi.org/10.1016/j.kint.2017.07.021.

Raubenheimer, E.J., Noffke, C.E., Mohamed, A., 2015. Expansive jaw lesions in chronic kidney disease: review of the literature and a report of two cases. Oral Surg. Oral Med. Oral Pathol. Oral Radiol. 119, 340–345. https://doi.org/10.1016/j.oooo.2014.11.002.

Schaffler, M.B., Burr, D.B., 1988. Stiffness of compact bone: effects of porosity and density. J. Biomech. 21, 13–16. https://doi.org/10.1016/0021-9290(88)90186-8.

Schött, E., Berge, O.G., Ängeby-Möller, K., Hammarström, G., Dalsgaard, C.J., Brodin, E., 1994. Weight bearing as an objective measure of arthritic pain in the rat. J. Pharmacol. Toxicol. Methods 31, 79–83. https://doi.org/10.1016/1056-8719(94)90046-9.

Tentori, F., McCullough, K., Kilpatrick, R.D., Bradbury, B.D., Robinson, B.M., Kerr, P.G., Pisoni, R.L., 2014. High rates of death and hospitalization follow bone fracture among hemodialysis patients. Kidney Int. 85, 166–173. https://doi.org/10.1038/ki.2013.279.

Vorland, C.J., Lachcik, P.J., Swallow, E.A., Metzger, C.E., Allen, M.R., Chen, N.X., Moe, S.M., Hill Gallant, K.M., 2019. Effect of ovariectomy on the progression of chronic kidney disease-mineral bone disorder (CKD-MBD) in female Cy/+ rats. Sci. Rep. 9, 1–8. https://doi.org/10.1038/s41598-019-44415-9.